

Supporting Information for ”A comparison of processing methods for the Oklahoma Lightning Mapping Array”

V. C. Chmielewski^{1,2} *, J. Blair^{1,2,3}, D. Kennedy², D. MacGorman¹, K. Calhoun²

¹Cooperative Institute for Severe and High-Impact Weather Research and Operations, University of Oklahoma, Norman, Oklahoma, U.S.A.

²NOAA/OAR National Severe Storms Laboratory, Norman, Oklahoma, U.S.A.

³School of Meteorology, University of Oklahoma, Norman, Oklahoma, U.S.A.

Contents of this file

1. Figures S1 to S5
2. Table S1

Additional Supporting Information (Files uploaded separately)

1. Captions for Movies S1 to S4

Corresponding author: V. C. Chmielewski, Cooperative Institute for Severe and High-Impact Weather Research and Operations, University of Oklahoma, 120 David L. Boren Blvd., Norman, Oklahoma, 73072, USA. (vanna.chmielewski@noaa.gov)

*120 David L. Boren Blvd., Norman, Oklahoma, 73072

Introduction

The table, image and video files included here provide additional perspectives on the VHF sources recorded by the OKLMA by each processing methodology as discussed in the text.

Figure S1 Analysis of all solutions in the separated method which were within x of a solution by the opposite cluster including where in the domain these events occurred (a), the distribution of how these events were separated from their match in three-dimensional distance or time (b), and the spatial distribution of the three-dimensional distance (c) and time (d) differences.

Figure S2 Histogram of the number of VHF sources by the number of contributing sensors from each cluster in the unified method from 0000 to 0600 UTC on 16 June 2019 with (a) reduced $\chi^2 \geq 1$ or altitudes ≥ 20 km which includes mostly noise and (b) reduced $\chi^2 < 1$ and altitudes < 20 km which includes more signal. Percentage of sources removed by time threshold at a constant distance threshold (c) and by distance threshold with constant time threshold (d). Black vertical line is the time (c) and distance (d) threshold used to select well-mapped potential duplicate sources as described in text.

Figure S3 Estimated flash detection efficiency (contour, %) and source detection efficiency (fill, %) following Chmielewski and Bruning 2016 for the central (a), southwest (b), unified (c), and combined (d) processing methods requiring a 6-station minimum per VHF source.

Figure S4 Same as Figure S3 but with a 7-station minimum.

Figure S5 VHF sources from the combined OKLMA processing method (colored by observing cluster) from 0429:02 to 0429:05 UTC on 16 June 2016 with reduced $\chi^2 \leq 1$

and at least 6 stations contributing to the source, as in Figure 1 with the spatial domain (f). Orange (blue) points are those mapped by the southwest (central) cluster. Larger points are those which would be eliminated and match with a source linked by a small black line.

Table S1 As in Table 1, but for Case 2 from 0300 to 0700 UTC.

Movie S1. Animation of all VHF sources from the unified OKLMA processing method (colored by time) from 0000 to 0559 UTC on 16 June 2016 with reduced $\chi^2 \leq 1$ and at least 7 stations contributing to the source. Sources are shown by (a) altitude and time, (b) altitude and longitude, (d) longitude and latitude and (e) latitude and altitude. (c) shows the histogram of source by altitude. The locations of OKLMA sensors are shown by the white diamonds. The analysis domain used is shown by the black box. Each frame contains 5 minutes of VHF sources.

Movie S2. As in Movie S1 but with the separated OKLMA processing method.

Movie S3. As in Movie S1 but for Case 2.

Movie S4. As in Movie S3 but with the separated OKLMA processing method.

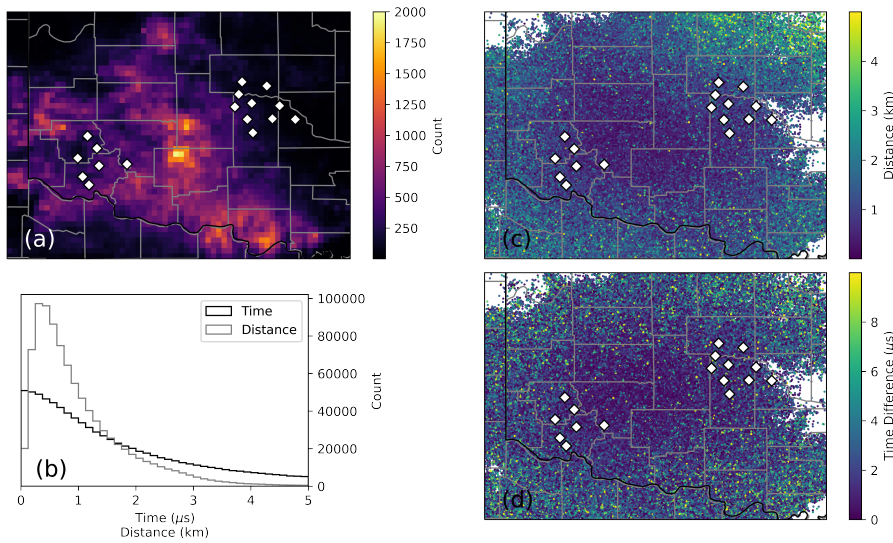


Figure S1. Analysis of all solutions in the separated method which were within x of a solution by the opposite cluster including where in the domain these events occurred (a), the distribution of how these events were separated from their match in three-dimensional distance or time (b), and the spatial distribution of the three-dimensional distance (c) and time (d) differences.

Table S1. As in Table 1, but for Case 2 from 0300 to 0700 UTC

	Unified	Separated	Duplicates Removed
Processing Time (min)	139.2	5.5	5.6
Total Count	29,538,290	20,119,375	19,737,811
Domain Count	24,761,756	19,331,153	18,951,993
$\leq 1 \chi^2$	18,327,944 (74.0)	15,855,421 (82.0)	15,536,470 (82.0)
≥ 7 stations	13,506,809 (54.5)	10,556,590 (54.6)	10,317,274 (54.4)
Count in flashes	17,153,588 (69.3)	15,325,314 (79.3)	15,006,381 (79.2)
Number of flashes	47,779	43,915	43,691
Average area (km ²)	54.86	57.27	57.24
Median area (km ²)	16.93	20.95	21.15

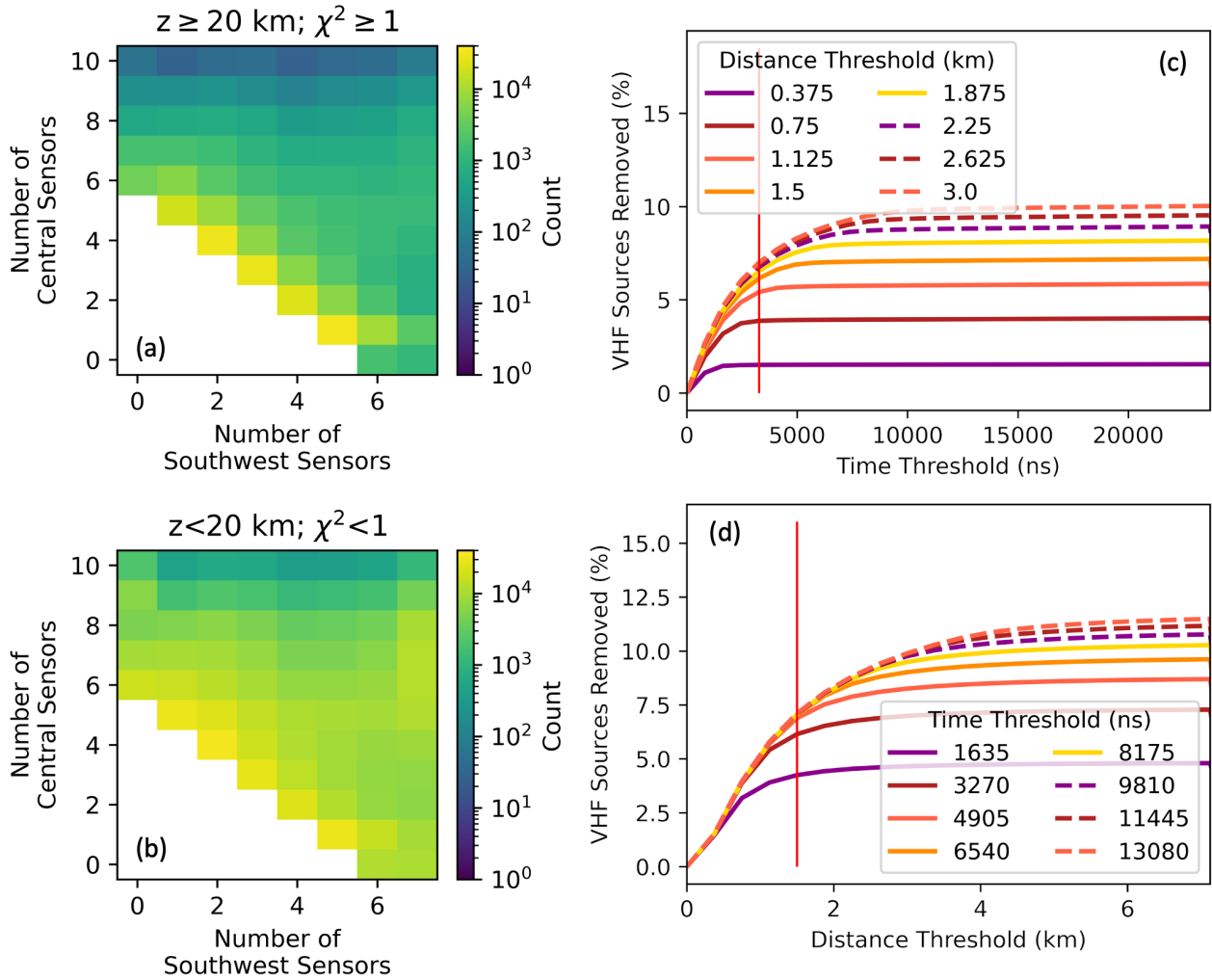


Figure S2. Histogram of the number of VHF sources by the number of contributing sensors from each cluster in the unified method from 0000 to 0600 UTC on 16 June 2019 with (a) reduced $\chi^2 \geq 1$ or altitudes ≥ 20 km which includes mostly noise and (b) reduced $\chi^2 < 1$ and altitudes < 20 km which includes more signal. Percentage of sources removed by time threshold at a constant distance threshold (c) and by distance threshold with constant time threshold (d). Black vertical line is the time (c) and distance (d) threshold used to select well-mapped potential duplicate sources as described in text.

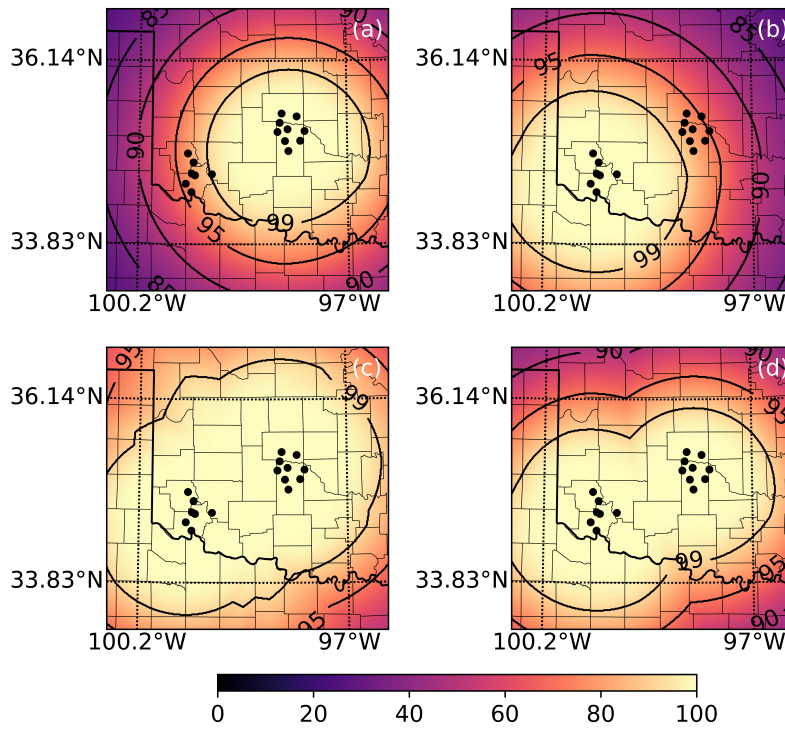


Figure S3. Estimated flash detection efficiency (contour, %) and source detection efficiency (fill, %) following Chmielewski and Bruning 2016 for the central (a), southwest (b), unified (c), and separated (d) processing methods requiring a 6-station minimum per VHF source.

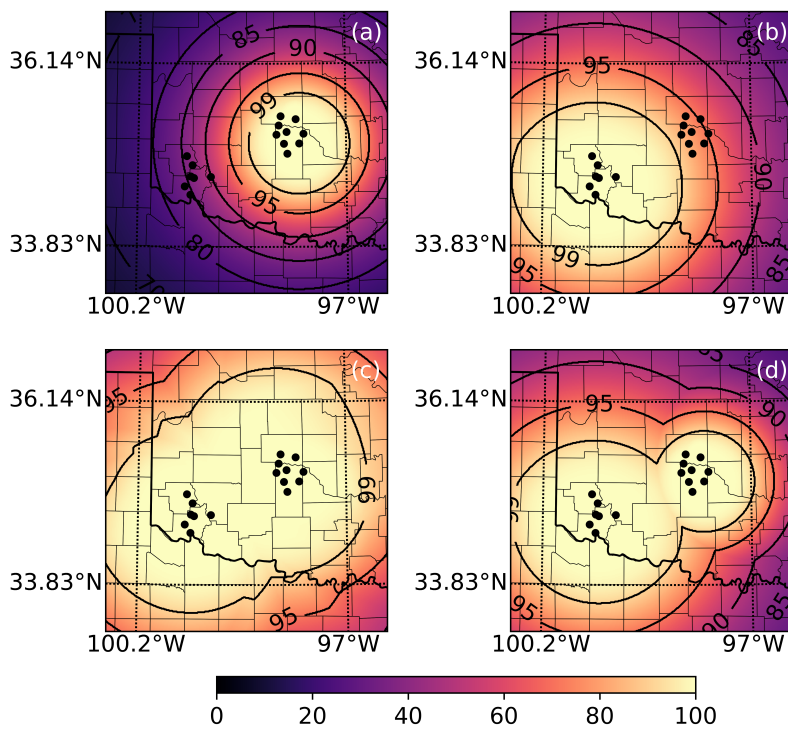


Figure S4. Same as Figure S3 but with a 7-station minimum.

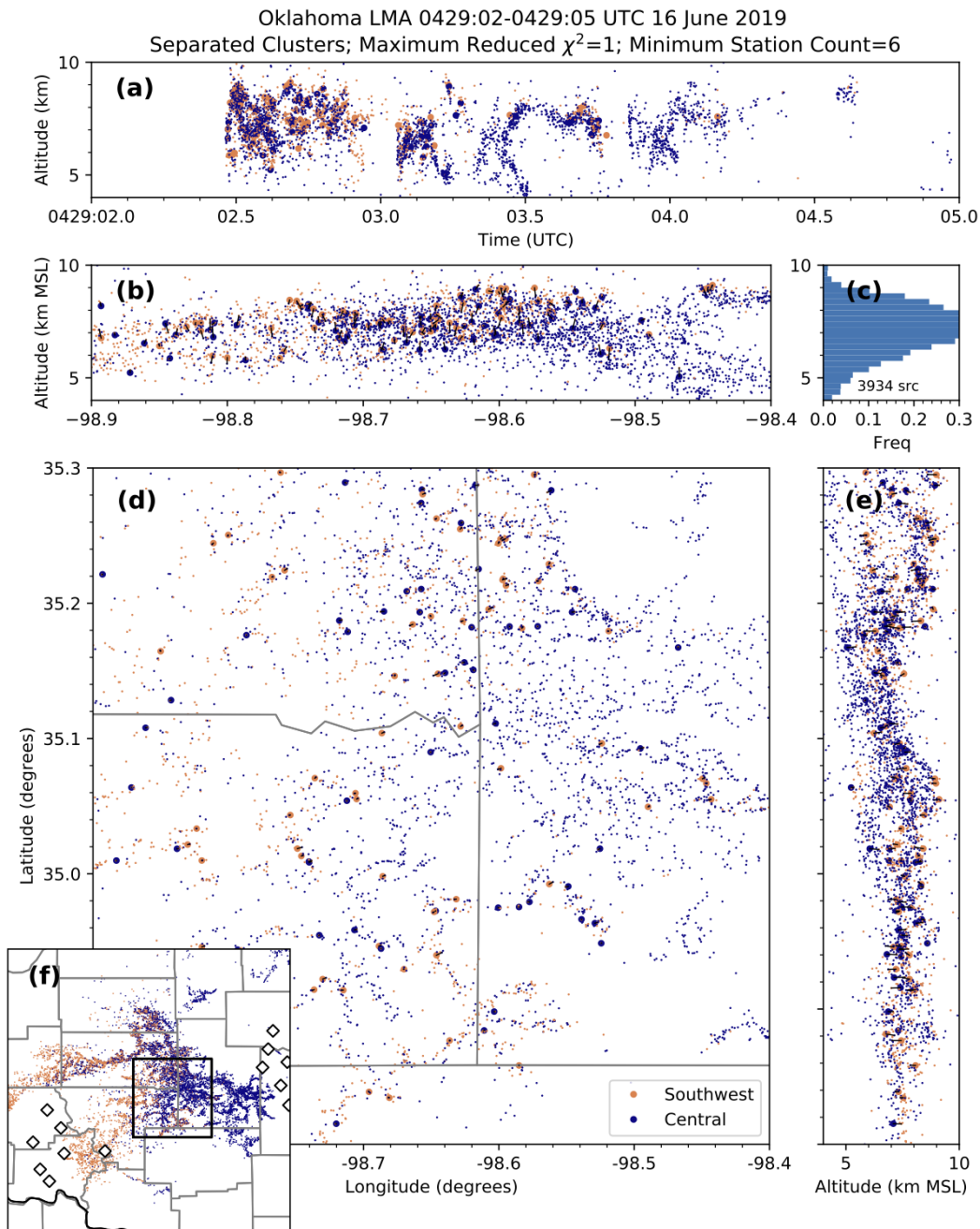


Figure S5. VHF sources from the combined OKLMA processing method (colored by observing cluster) from 0429:02 to 0429:05 UTC on 16 June 2016 with reduced $\chi^2 \leq 1$ and at least 6 stations contributing to the source, as in Figure 1 with the spatial domain (f). Orange (blue) points are those mapped by the southwest (central) cluster. Larger points are those which would be eliminated and match with a source linked by a small black line.

February 2, 2022, 11:44pm